First-Order Fibre Bragg Grating Inscription in Indium Fluoride Fibre using UV/Vis Femtosecond Laser and Two-Beam Interferometry

ISMAEL CHIAMENTI[1,2,*], TINO ELSMANN[1], AARON REUPERT[3], OGUZHAN KARA[1], MARTIN BECKER[1], LOTHAR WONDRACZEK[3], AND MARIA CHERNYSHEVA[1]

[1] Leibniz Institute of Photonic Technology, Leibniz-IPHT, Albert-Einstein-Straße 9, 07745 Jena, Germany
[2] Federal University of Technology - Paraná - UTFPR/DAELT, Av. Sete de Setembro 3165, 80230-901 Curitiba, Brazil
[3] Otto Schott Institute of Materials Research, Friedrich Schiller University, 07743 Jena, Germany
[*] chiamenti@utfpr.edu.br

Compiled March 11, 2021

Fibre gratings are among key components in fibre-based photonics systems and, particularly, laser cavities. In latter, they can play multiple roles, such as those of mirrors, polarisers, filters or dispersion compensators. In this Letter, we present the inscription of highly reflective first-order fibre Bragg gratings (FBGs) in soft indium fluoride-based (InF_3) fibres using a two-beam phase-mask interferometer and a femtosecond laser. We demonstrate an enhanced response of InF_3-based fibre to a visible (400 nm) inscription wavelength compared to ultraviolet irradiation at 266 nm. In this way, FBGs with a reflectivity of over 99.7% were inscribed at around 1.9 µm with the bandwidth of 2.68 nm. After thermal annealing at 393 K, the Bragg wavelength demonstrates stable thermal shift of 20 pm/K in the temperature range spanning from 293 to 373 K. These observations suggest a potential extension of InF_3 fibre-based laser components to an operational range of up to 5 µm.

http://dx.doi.org/10.1364/ao.XX.XXXXXX

Fibre laser technology has become a versatile solution for different applications in Near- [1, 2] and Short-wave-infrared wavelength ranges [3]. Their benefits such as high beam quality, outstanding stability, excellent thermal management, alignment-free operation, robustness and design flexibility have enabled widespread use and continuous research and development. Mid-infrared (Mid-IR) fibre lasers have gained research attention as their emission wavelength matches the vibrational modes of molecules. They can be used for chemical and environmental sensing and diagnostics [4–7], but also in micromachning [4] and laser surgery [8], or LIDARs in the low-loss atmospheric windows [6, 9]. However, due to high phonon energy ($\sim$1100 cm^{-1}) and, therefore, high absorption losses, conventional silica-based fibre technology cannot be transferred to the wavelength ranges beyond 2.5 µm. For this reason, the state-of-the-art fibre materials have been expanded towards soft glasses, such as fluorides and chalcogenides (sulfide, selenide and telluride) [10]. Among these, zirconium-fluoride-based fibres, mainly ZBLAN (ZrF_4-BaF_2-LaF_3-AlF_3-NaF), are the most mature and have enabled laser generation up to 3.9 µm, when doped with holmium ions (Ho^{3+}) [11], and supercontinuum generation spanning from 1.9 µm to 4.5 µm [12]. Still, the operational wavelength range of ZBLAN fibres is limited to about 3.8 µm. Thus, recently developed InF_3-based fibres present a promising alternative to ZBLAN, as they feature a wider transmission range of up to 5 µm [13], which allows pushing the laser emission wavelength beyond 4 µm, when doped with erbium or dysprosium ions [14, 15]. Despite recent advances in achieving direct Mid-IR generation, the demonstrated fibre lasers still included bulk components, which set some major constraints on the optical design compared to all-fibre configurations.

A potential solution for obtaining some of the fibre-based components is the fabrication of fibre integrated gratings: fibre Bragg gratings (FBG), chirped FBG (CFBG), long-period gratings (LPG), tilted FBGs (TFBG). FBGs are widely used as high and low reflective mirrors to create robust laser cavities [16]. Grating structures such as TFBGs, CFBGs, and LPGs can be used as polarisers [17], filters [18], or for dispersion compensation [19]. Up to date, however, just a few studies have demonstrated successful FBGs inscription in ZBLAN, and only recently the first such demonstration was made for InF_3-based fibres. The inscription was mainly done by using IR or Vis femtosecond (fs)-lasers for step-by-step (point-by-point, line-by-line, plane-by-plane) inscription techniques [20, 21]. The inscription technique utilising UV-laser interference, prevailing for silica fibres, cannot be applied directly to pure ZBLAN glasses due to their low photosensitivity to UV irradiation. Such an inscription requires additional dopants to the glass matrix, such as cerium in order to enhance the photosensitivity [22]. Despite high flexibility of grating designs produced using step-by-step inscription technique [23], it requires highly precise motorised stage systems, which determine the reproducibility of the resulting grating properties. The inscription process is, therefore, quite elaborate. At the same time, post-processing of fluoride fibres introduces even more limitations, such as the narrow operational window of pulse energy and inscription speed to avoid damage of the soft fibres. Remarkably high FBG reflectivity of 95.2% has been demonstrated in second-order gratings after thermal annealing in [21]. Nevertheless, first-order FBGs are supposed to feature higher reflectivity, particularly, at longer wavelengths [21].

In this work, we present the inscription of highly refractive first-

order FBGs in passive InF_3-based fibres, using a two-beam phase-mask interferometer and a fs-laser operating at 266 and 400 nm. The results show successful first-order FBGs inscription in InF_3-based fibres at around 1.9 µm with a reflectivity higher than 99.7%, high symmetry and side-lobe suppression higher than 25 dB when using Vis light irradiation. We have performed thermal treatment and investigated the temperature response and stability of the FBGs. The FBGs feature high thermal stability and low loss over a wide spectral range. The versatility of the interferometer inscription technique does not pose any restrictions for translating the technique to even longer wavelength ranges as long as a corresponding phase mask is available. Therefore, the demonstrated results provide the ground for developing tailored InF_3 fibre-based components and, thus, boosting Mid-IR laser performance.

The FBG inscription system was based on a two-beam phase-mask interferometer (Fig. 1 a) with a Ti:Sapphire fs-laser (Coherent Inc). The laser was combined with Beta-Barium Borate (BBO) crystals to enable emission of 350-fs pulses at 266 or 400 nm. The inscription laser beam featured a width at half-maximum (FWHM) of around 7 mm. It was focused into the fibre core by a cylindrical lens with a focal length of 390 mm in the case of the inscription at 266 nm, and 408 mm – for 400 nm laser wavelength. The resulting cross-sectional area of the inscription laser beam in the fibre core was approximately 7×0.01 mm^2. Two phase masks (Ibsen Photonics) were optimised to minimise the zero-order diffraction at the inscription wavelengths (UV or Vis). The residual energy of this order was blocked. Both phase masks had a pitch of 1379 nm. The interferometer mirrors combine the ±1 orders of the phase mask to produce an interference pattern. This pattern was inscribed into the fibre core trough the refractive index modification by the fs-laser and had the period Λ determined as [24]:

$$\Lambda(\delta) = \frac{\lambda_{\text{insc}}}{2\sin\left(\arcsin\left(\frac{\lambda_{\text{insc}}}{\Lambda_{\text{PM}}}\right)+2\delta\right)} \quad (1)$$

, where λ_{insc} is the inscription wavelength of the fs-laser, Λ_{PM} is the period (pitch) of the phase mask used as a beam splitter, and δ is the angular position of the interferometer's mirrors. The mirror alignment determines Bragg wavelength as $\lambda_{\text{Bragg}}(\delta) = 2n_{\text{eff}}\Lambda(\delta)$, where n_{eff} is the effective refractive index of the reflected mode. In the experiment, the phase mask was selected, and the setup was aligned for FBG inscription with λ_{Bragg} around 1.9 µm, restricted by the available measurement equipment. In contrast to the direct phase mask inscription, the interferometric technique allows tuning the Bragg wavelength λ_{Bragg} within at least ±100 nm range by rotating the mirrors.

The FBGs were inscribed in a passive indium fluoride fibre (Le Verre Fluoré) with a core diameter of 7.5 µm and the numerical aperture of 0.3. The fibre glass composition is based on indium fluoride and several other fluorides, such as BaF_2, SrF_2, CaF_2, PbF_2 [25]. The FBG reflection and transmission spectra were characterised using a broadband light source at around 1.9 µm (AdValue AP-ASE-2000-SM) connected through a fibre optic circulator, and an optical spectrum analyser (Yokogawa AQ6375). The reflectivity of FBGs was estimated from the transmission spectra. The InF_3-based fibre was connected to SMF-28 fibre patch cords via FC-PC connectors. The cut-off wavelength of the InF_3 fibre was 2.95 μm, therefore, it effectively guides two modes at chosen Bragg wavelength. However, only negligible portion of the fundamental mode, launched from SMF-28 fibre, was coupled into the second mode within the short InF_3-based fibre lengths (around 1 m). Therefore, the presented results demonstrate the FBG properties for the fundamental mode.

By using the described methodology, a series of FBGs was inscribed at different conditions. FBG#1 was inscribed with the fs-laser operating at 266 nm with 120 mW average power at 1 kHz repetition rate. Additionally, a 1 Hz shutter was used during UV-fs-laser inscription,

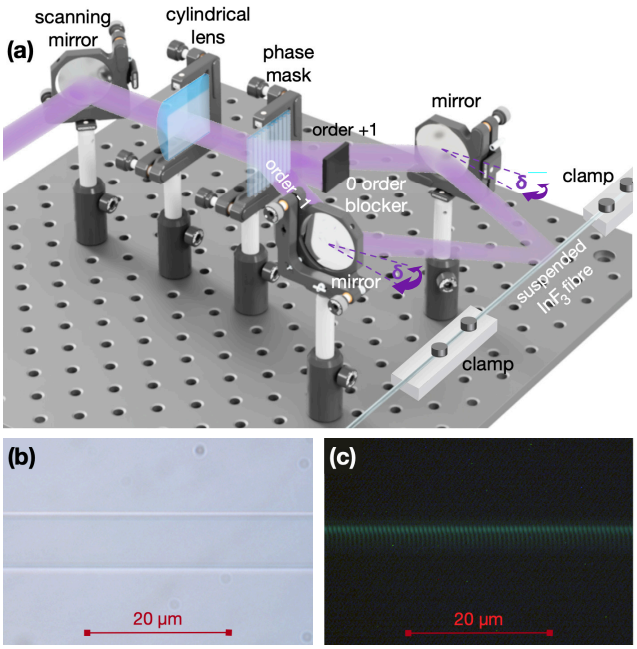

Fig. 1. (a) Principle of FBG interferometric inscription setup; (b) bright- and (c) dark-field images of the FBG in InF_3-based fibre.

reducing laser exposure to only 100 ms per second. This prevented fibre bending due to heat accumulation during laser exposure. The total inscription time was around 4 hours. Fig. 2 (a) shows the FGB#1 reflection and transmission spectra with the reflection of ~55%.

Compared to the step-by-step inscription, the FBGs fabricated using phase mask techniques feature much smaller modification of the fibre core refractive index. Therefore, Bragg gratings are generally invisible in standard bright-field microscopy, as shown in Fig. 1 (b). To improve the image contrast, a green laser diode (wavelength 520 nm) was coupled to the fibre, whereby imaging was done without microscope illumination [26], similarly to the dark-field microscopy technique (Fig. 1 c). Such methodology has the advantage that the primary beam remains contained within the fibre and only the scattered or diffracted light from the grating is collected by the objective. Both images in Fig. 1 (b,c) were made using paraffin oil immersion with the refractive index of $n = 1.467$, which is close to the fibre cladding, and a microscope (Zeiss JenaPol Interphako, numerical aperture (NA) 1.35 and 100 times magnification objective). The grating period of 655 nm (123 periods on 80.6 µm) from the dark-field image in Fig. 1 (c) is in good agreement with the estimate, calculated through Eq. 1.

Due to rapidly increasing absorption in InF_3-based fibres in the UV range, the required long exposure to the fs-laser light at 266 nm causes a substantial thermal load, which was only partially mitigated by the shutter. Such a critical thermal load leads to mechanical instabilities during the inscription, reducing the quality of the FBGs and limiting its reflectivity intensity. Therefore, the fs-laser 400 nm wavelength was used to investigate the inscription of FBGs with higher reflectivity. Since the InF_3-based fibre absorption is more than 20 dB/m smaller at 400 nm than at 266 nm, the additional shutter is no longer required. Therefore, the inscription at the visible range would be realised by ten times as many pulses as at UV irradiation, thus, can increase the inscription efficiency.

FBG#2 was inscribed with the fs-laser operating at 400 nm with the average power of 100 mW at 1 kHz-repetition rate, with a total exposure time of 1 hour. The average power increase above 100 mW resulted in heat accumulation, which caused fibre bending, as previously described.

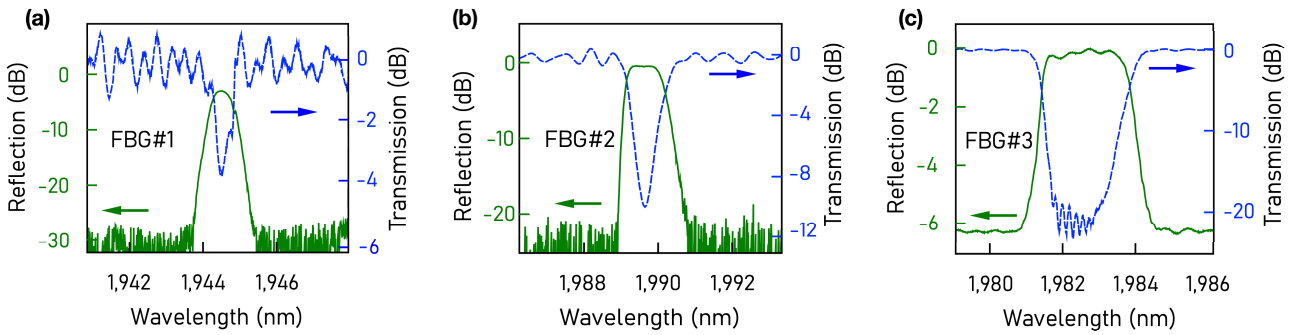

Fig. 2. Reflection (green trace) and transmission (blue dashed trace) spectra of FBGs inscribed using (a) 266 nm and (b-c) 400 nm fs-laser

The reflectivity of the inscribed FBG was limited to only 90% (Fig. 2 b).

To decrease the mechanical instability of the inscription process further, the fibre clamps (shown in Fig. 1 a) were positioned closer to each other, reducing the length of a suspended section of the fibre. Thereby, FBG#3 was inscribed with the fs-laser operating at 400 nm, 100 mW average power and 1 kHz repetition rate, with a total exposure time of 2 hours. As shown in Fig. 2 (c), FBG#3 features reflectivity higher than 99.7%. The difference in the reflection baseline between the spectra of FBG#3 and other FBGs in Fig. 2 is due to improper fibre connectorisation of InF_3-based fibre.

To investigate the thermal properties of the inscribed FBGs, first, they were thermally annealed by heating to 393 K. Figures 3 (a-c) show temperature profile and evolution of FBGs#1 and 3 Bragg wavelength during annealing process. With the temperature rise, the expected red-shift (by ∼1.6 nm) of the Bragg wavelengths occurred. FBGs were kept at the high temperature until the velocity of the Bragg wavelength shift decay was nearly constant. The decay was assessed over two time intervals, particularly, 30 min and 1 hour. When the reflected Bragg wavelength shift reached a decaying ratio of less then -20 pm/h and -10 pm/30 min simultaneously, the fibres were cooled down to

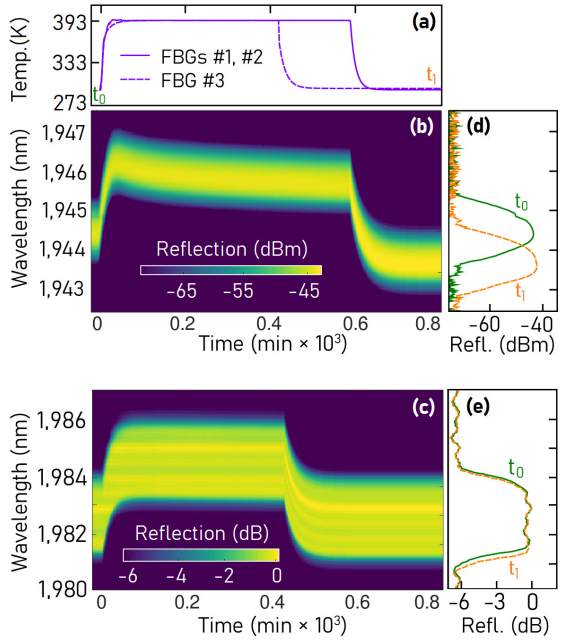

Fig. 3. (a) Temperature profile of the thermal treatment, (b-c) map of Bragg wavelength shift and (d-e) reflection spectra before and after the thermal treatment for FBGs#1 and #3, respectively.

Table 1. Fibre Bragg gratings parameters variation induced by thermal treatment

FBG	$\Delta\lambda_{Bragg}$, pm	ΔFWHM, pm	ΔReflec.	$\Delta n_{\text{eff}} \times 10^{-4}$
#1	−765(−0.039%)	+50(+8.5%)	+28.7%	-5.9
#2	−795(−0.040%)	+10(+1.0%)	+16.4%	-6.0
#3	−120(−0.006%)	+100(+3.7%)	< 1%	-0.9

room temperature. It is worth noting that FBG#3 got stabilised much faster than its counterparts. After cooling down to room temperature, permanent changes in FBGs spectra were observed. FBG#1 (Fig. 3 d) exhibited a stronger blue-shift of the Bragg wavelength and a greater reflection intensity increase compared to FBG#3 (Fig. 3 e). It was also detected that the FWHM and the reflectivity for all the three FBGs increased as a result of thermal treatment. We attribute these changes to the reduction of parasitic defects within the grating, *e.g.* the fast annealing of weak defects in the grating minima compared to the more stable saturated defects in the maxima. Alteration of FBGs parameters, resulting from thermal treatment, are compiled in Table 1.

The blue shift in the Bragg wavelengths can be interpreted as a reduction of the effective refractive index n_{eff} of the gratings after the thermal treatment [27]. Table 1 presents the estimate change in n_{eff} from the Bragg wavelength assuming the grating period to be constant. The relative decrease of FBG#1 and FBG#2 refractive index was almost 60×10^{-5} but for FBG#3 only 9×10^{-5} with a measurement uncertainty of less than 2×10^{-5}. The different behaviour of FBGs during thermal annealing and blue shift of their Bragg wavelengths can indicate different mechanisms that modify the fibre core refractive index of InF_3-based fibre. These mechanisms might result in the formation of diverse gratings structures, similar to Bragg grating types I, II, II_A, *etc.*, in silica optical fibres [28].

After thermal annealing, the thermal response and stability of the FBGs were investigated. The InF_3-based fibre sections with the FBGs were subjected to five heating-cooling cycles with temperature variation of 293–373 K with 10 K step. Figure 4 (a) shows the results of the thermal cycling experiment for FBG#2. Nearly no hysteresis was observed due to the prior annealing. The experimental data were fitted with a linear equation, demonstrating a temperature sensitivity of around 20 pm/K, which is almost twice as high as of FBG's in silica fibres [29]. Other inscribed FBGs showed similar sensitivity. Such thermal stability and response are beneficial for sensing application, as well as for laser development, *e.g.* for ensuring tuneability or stabilisation of systems.

Previous studies on FBGs inscribed in fluoride fibres demonstrated significant losses (up to 3.7 dB) induced by gratings [30], restricting

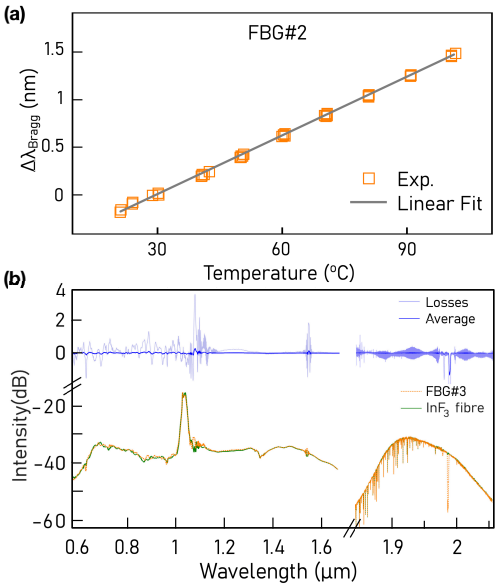

Fig. 4. (a) Thermal response of FBG#2 after the thermal treatment and (b) Broadband spectra transmitted through InF_3 fibre with and without FBG#3 and estimated losses (blue plots).

their applications in high-power lasers. We investigated the losses caused by FBG#3 inscription in the wavelength range of 600 to 2050 nm (with the exception to 1,700-1,840 nm range due to light source unavailability), which covers important bands of laser pump wavelength and emission (Fig. 4 b). The losses were measured immediately after the FBGs inscription and after thermal treatment. As it is seen from the averaged loss spectrum in Fig. 4 (b), even with the typical noisy signal from the supercontinuum light source the FBG-induced average losses are at a maximum in the order of 0.1 dB, which is an acceptable value for further application of such FBGs *e.g.* in fibre laser development. Moreover, the thermal treatment does not introduce any change in the spectrum of optical losses.

In summary, we presented the inscription of highly reflective first-order FBGs in passive indium fluoride optical fibres using a two-beam phase-mask interferometer and a fs-laser. Due to the availability of laser source and measurement equipment, the reflection of FBGs was centred at around 1.9 µm. However, with the fabrication of tailored phase mask, the demonstrated FBG inscription technology can be adapted with no limitation to longer wavelength ranges within the transparency region of InF_3-based optical fibres.

We have compared the FBGs inscription processes using fs-laser irradiation at 266 and 400 nm. The application of the visible inscription wavelength has produced a stable first-order FBGs with more then 99.7% reflectivity. The FBGs demonstrate low insertion losses of ≤ 0.1 dB, measured over a broad spectral region, spanning from 600 to 2050 nm. We have also observed almost linear thermal sensitivity of FBGs in InF_3-based fibres of 20 pm/K and thermal stability after annealing at 393 K. The small losses and the spectral quality of the FBGs will contribute to the development of the advanced photonic systems, and particularly, all-fibre lasers operating in the Mid-IR range within the transparency window of InF_3-based optical fibre up to 5 µm.

ACKNOWLEDGMENTS

I. C. kindly thanks the Leibniz-IPHT for welcoming him as visiting researcher. L.W. acknowledges support of Carl Zeiss Foundation within its Breakthrough Program.

Disclosures. The authors declare no conflicts of interest.

REFERENCES

1. J. Rothhardt, S. Hädrich, J. Delagnes, E. Cormier, and J. Limpert, Laser & Photonics Rev. **11**, 1700043 (2017).
2. J. D. Bradley and M. Pollnau, Laser & Photonics Rev. **5**, 368 (2011).
3. D. Kirsch, S. Chen, R. Sidharthan, Y. Chen, S. Yoo, and M. Cherny-sheva, J. Appl. Phys. **128**, 180906 (2020).
4. A. Schliesser, N. Picqué, and T. W. Hänsch, Nat. Photonics **6**, 440 (2012).
5. A. B. Seddon, B. Napier, I. Lindsay, S. Lamrini, P. M. Moselund, N. Stone, O. Bang, and M. Farries, The Analyst **143**, 5874 (2018).
6. P. M. Moselund, C. Petersen, S. Dupont, C. Agger, O. Bang, and S. R. Keiding, "Supercontinuum: broad as a lamp, bright as a laser, now in the mid-infrared," in *Laser Technology for Defense and Security VIII,* (SPIE, 2012).
7. J. S. Li, W. Chen, and H. Fischer, Appl. Spectrosc. Rev. **48**, 523 (2013).
8. S. Amini-Nik, D. Kraemer, M. L. Cowan, K. Gunaratne, P. Nadesan, B. A. Alman, and R. D. Miller, PLoS one **5**, e13053 (2010).
9. V. Mitev, S. Babichenko, J. Bennes, R. Borelli, A. Dolfi-Bouteyre, L. Fiorani, L. Hespel, T. Huet, A. Palucci, M. Pistilli, A. Puiu, O. Rebane, and I. Sobolev, "Mid-IR DIAL for high-resolution mapping of explosive precursors," in *Lidar Technologies, Techniques, and Measurements for Atmospheric Remote Sensing IX,* U. N. Singh and G. Pappalardo, eds. (SPIE, 2013).
10. G. Tao, H. Ebendorff-Heidepriem, A. M. Stolyarov, S. Danto, J. V. Badding, Y. Fink, J. Ballato, and A. F. Abouraddy, Adv. Opt. Photonics **7**, 379 (2015).
11. J. Schneider, Electron. Lett. **31**, 1250 (1995).
12. O. P. Kulkarni, V. V. Alexander, M. Kumar, M. J. Freeman, M. N. Islam, J. Fred L. Terry, M. Neelakandan, and A. Chan, J. Opt. Soc. Am. B **28**, 2486 (2011).
13. R. Salem, Z. Jiang, D. Liu, R. Pafchek, D. Gardner, P. Foy, M. Saad, D. Jenkins, A. Cable, and P. Fendel, Opt. Express **23**, 30592 (2015).
14. F. Maes, V. Fortin, S. Poulain, M. Poulain, J.-Y. Carrée, M. Bernier, and R. Vallée, Optica **5**, 761 (2018).
15. M. R. Majewski, R. I. Woodward, J.-Y. Carreé, S. Poulain, M. Poulain, and S. D. Jackson, Opt. Lett. **43**, 1926 (2018).
16. N. Jovanovic, A. Fuerbach, G. D. Marshall, M. J. Withford, and S. D. Jackson, Opt. Lett. **32**, 1486 (2007).
17. K. Feder, P. Westbrook, J. Ging, P. Reyes, and G. Carver, IEEE Photonics Technol. Lett. **15**, 933 (2003).
18. A. Vengsarkar, P. Lemaire, J. Judkins, V. Bhatia, T. Erdogan, and J. Sipe, J. Light. Technol. **14**, 58 (1996).
19. R. Kashyap, S. Chernikov, J. Taylor, and P. McKee, Electron. Lett. **30**, 1078 (1994).
20. A. Fuerbach, G. Bharathan, and M. Ams, IEEE Photonics J. **11**, 1 (2019).
21. G. Bharathan, T. T. Fernandez, M. Ams, J.-Y. Carrée, S. Poulain, M. Poulain, and A. Fuerbach, Opt. Lett. **45**, 4316 (2020).
22. T. Taunay, H. Poignant, S. Boj, P. Niay, P. Bernage, E. Delevaque, M. Monerie, and E. X. Xie, Opt. Lett. **19**, 1269 (1994).
23. G. D. Marshall, R. J. Williams, N. Jovanovic, M. J. Steel, and M. J. Withford, Opt. Express **18**, 19844 (2010).
24. M. Becker, J. Bergmann, S. Brückner, M. Franke, E. Lindner, M. W. Rothhardt, and H. Bartelt, Opt. Express **16**, 19169 (2008).
25. G. Maze, M. Poulain, J. Carre, A. Soufiane, and Y. Messaddeq, "Fluorinated glasses," in *U. S. Patent, No. 5,480,845,* (United States Patent, 1996).
26. A. Reupert, M. Heck, S. Nolte, and L. Wondraczek, Adv. Opt. Mater. **8**, 2000633 (2020).
27. A. Munko, S. Arkhipov, A. Gribaev, K. Konnov, M. Belikin *et al.*, J. Physics: Conf. Ser. **735**, 012015 (2016).
28. R. Kashyap, *Fiber Bragg Gratings* (Academic Press, 1999).
29. A. Othonos and K. Kalli, *Fiber Bragg gratings: Fundamentals and Applications in Telecommunications and Sensing* (Artech House, 1999).
30. F. Maes, C. Stihler, L.-P. Pleau, V. Fortin, J. Limpert, M. Bernier, and R. Vallée, Opt. Express **27**, 2170 (2019).

FULL REFERENCES

1. J. Rothhardt, S. Hädrich, J. Delagnes, E. Cormier, and J. Limpert, "High average power near-infrared few-cycle lasers," Laser & Photonics Rev. **11**, 1700043 (2017).
2. J. D. Bradley and M. Pollnau, "Erbium-doped integrated waveguide amplifiers and lasers," Laser & Photonics Rev. **5**, 368–403 (2011).
3. D. Kirsch, S. Chen, R. Sidharthan, Y. Chen, S. Yoo, and M. Chernysheva, "Short-wave IR ultrafast fiber laser systems: Current challenges and prospective applications," J. Appl. Phys. **128**, 180906 (2020).
4. A. Schliesser, N. Picqué, and T. W. Hänsch, "Mid-infrared frequency combs," Nat. Photonics **6**, 440–449 (2012).
5. A. B. Seddon, B. Napier, I. Lindsay, S. Lamrini, P. M. Moselund, N. Stone, O. Bang, and M. Farries, "Prospective on using fibre mid-infrared supercontinuum laser sources for in vivo spectral discrimination of disease," The Analyst **143**, 5874–5887 (2018).
6. P. M. Moselund, C. Petersen, S. Dupont, C. Agger, O. Bang, and S. R. Keiding, "Supercontinuum: broad as a lamp, bright as a laser, now in the mid-infrared," in *Laser Technology for Defense and Security VIII,* (SPIE, 2012).
7. J. S. Li, W. Chen, and H. Fischer, "Quantum cascade laser spectrometry techniques: A new trend in atmospheric chemistry," Appl. Spectrosc. Rev. **48**, 523–559 (2013).
8. S. Amini-Nik, D. Kraemer, M. L. Cowan, K. Gunaratne, P. Nadesan, B. A. Alman, and R. D. Miller, "Ultrafast mid-ir laser scalpel: protein signals of the fundamental limits to minimally invasive surgery," PLoS one **5**, e13053 (2010).
9. V. Mitev, S. Babichenko, J. Bennes, R. Borelli, A. Dolfi-Bouteyre, L. Fiorani, L. Hespel, T. Huet, A. Palucci, M. Pistilli, A. Puiu, O. Rebane, and I. Sobolev, "Mid-IR DIAL for high-resolution mapping of explosive precursors," in *Lidar Technologies, Techniques, and Measurements for Atmospheric Remote Sensing IX,* U. N. Singh and G. Pappalardo, eds. (SPIE, 2013).
10. G. Tao, H. Ebendorff-Heidepriem, A. M. Stolyarov, S. Danto, J. V. Badding, Y. Fink, J. Ballato, and A. F. Abouraddy, "Infrared fibers," Adv. Opt. Photonics **7**, 379 (2015).
11. J. Schneider, "Fluoride fibre laser operating at 3.9 µm," Electron. Lett. **31**, 1250–1251 (1995).
12. O. P. Kulkarni, V. V. Alexander, M. Kumar, M. J. Freeman, M. N. Islam, J. Fred L. Terry, M. Neelakandan, and A. Chan, "Supercontinuum generation from ~1.9 to 4.5 μm in ZBLAN fiber with high average power generation beyond 3.8 μm using a thulium-doped fiber amplifier," J. Opt. Soc. Am. B **28**, 2486 (2011).
13. R. Salem, Z. Jiang, D. Liu, R. Pafchek, D. Gardner, P. Foy, M. Saad, D. Jenkins, A. Cable, and P. Fendel, "Mid-infrared supercontinuum generation spanning 18 octaves using step-index indium fluoride fiber pumped by a femtosecond fiber laser near 2μm," Opt. Express **23**, 30592 (2015).
14. F. Maes, V. Fortin, S. Poulain, M. Poulain, J.-Y. Carrée, M. Bernier, and R. Vallée, "Room-temperature fiber laser at 3.92μm," Optica **5**, 761 (2018).
15. M. R. Majewski, R. I. Woodward, J.-Y. Carreé, S. Poulain, M. Poulain, and S. D. Jackson, "Emission beyond 4 μm and mid-infrared lasing in a dysprosium-doped indium fluoride (InF3) fiber," Opt. Lett. **43**, 1926 (2018).
16. N. Jovanovic, A. Fuerbach, G. D. Marshall, M. J. Withford, and S. D. Jackson, "Stable high-power continuous-wave Yb^{3+}-doped silica fiber laser utilizing a point-by-point inscribed fiber Bragg grating," Opt. Lett. **32**, 1486 (2007).
17. K. Feder, P. Westbrook, J. Ging, P. Reyes, and G. Carver, "In-fiber spectrometer using tilted fiber gratings," IEEE Photonics Technol. Lett. **15**, 933–935 (2003).
18. A. Vengsarkar, P. Lemaire, J. Judkins, V. Bhatia, T. Erdogan, and J. Sipe, "Long-period fiber gratings as band-rejection filters," J. Light. Technol. **14**, 58–65 (1996).
19. R. Kashyap, S. Chernikov, J. Taylor, and P. McKee, "30 ps chromatic dispersion compensation of 400 fs pulses at 100 gbits/s in optical fibres using an all fibre photoinduced chirped reflection grating," Electron. Lett. **30**, 1078–1080 (1994).
20. A. Fuerbach, G. Bharathan, and M. Ams, "Grating inscription into fluoride fibers: A review," IEEE Photonics J. **11**, 1–11 (2019).
21. G. Bharathan, T. T. Fernandez, M. Ams, J.-Y. Carrée, S. Poulain, M. Poulain, and A. Fuerbach, "Femtosecond laser direct-written fiber bragg gratings with high reflectivity and low loss at wavelengths beyond 4 ¯m," Opt. Lett. **45**, 4316 (2020).
22. T. Taunay, H. Poignant, S. Boj, P. Niay, P. Bernage, E. Delevaque, M. Monerie, and E. X. Xie, "Ultraviolet-induced permanent bragg gratings in cerium-doped ZBLAN glasses or optical fibers," Opt. Lett. **19**, 1269 (1994).
23. G. D. Marshall, R. J. Williams, N. Jovanovic, M. J. Steel, and M. J. Withford, "Point-by-point written fiber-Bragg gratings and their application in complex grating designs," Opt. Express **18**, 19844 (2010).
24. M. Becker, J. Bergmann, S. Brückner, M. Franke, E. Lindner, M. W. Rothhardt, and H. Bartelt, "Fiber Bragg grating inscription combining DUV sub-picosecond laser pulses and two-beam interferometry," Opt. Express **16**, 19169 (2008).
25. G. Maze, M. Poulain, J. Carre, A. Soufiane, and Y. Messaddeq, "Fluorinated glasses," in *U. S. Patent, No. 5,480,845,* (United States Patent, 1996).
26. A. Reupert, M. Heck, S. Nolte, and L. Wondraczek, "Angular scattering pattern of femtosecond laser-induced refractive index modifications in optical fibers," Adv. Opt. Mater. **8**, 2000633 (2020).
27. A. Munko, S. Arkhipov, A. Gribaev, K. Konnov, M. Belikin *et al.*, "The study of the thermal annealing of the bragg gratings induced in the hydrogenated birefringent optical fiber with an elliptical stress cladding," J. Physics: Conf. Ser. **735**, 012015 (2016).
28. R. Kashyap, *Fiber Bragg Gratings* (Academic Press, 1999).
29. A. Othonos and K. Kalli, *Fiber Bragg gratings: Fundamentals and Applications in Telecommunications and Sensing* (Artech House, 1999).
30. F. Maes, C. Stihler, L.-P. Pleau, V. Fortin, J. Limpert, M. Bernier, and R. Vallée, "3.42μm lasing in heavily-erbium-doped fluoride fibers," Opt. Express **27**, 2170 (2019).